Trees (2024) 38:1137–1150
https://doi.org/10.1007/s00468-024-02541-6

ORIGINAL ARTICLE

Responses of wood formation to bending: a matter of dose and sensitivity adjustments

Jeanne Roignant[1] · Éric Badel[1] · Nathalie Leblanc-Fournier[1] · Nicole Brunel-Michac[1] · Julien Ruelle[2] · Bruno Moulia[1] · Mélanie Decourteix[1]

Received: 5 September 2023 / Accepted: 24 June 2024 / Published online: 2 July 2024

Abstract

Key message **Repeated bending stimulations applied on poplar stem drives wood formation toward egg-shaped cross sections, thicker fiber cell walls and more fibers developing a G-layer; but cells sensitivity accommodates to avoid overresponses.**

Abstract Trees acclimate to mechanical stimulations (e.g. wind) through thigmomorphogenesis. Recent studies have demonstrated that repetitive unidirectional bending treatments applied to poplar stems result in the production of two distinct types of wood: tensile flexure wood (TFW) on the stretched side and compressive flexure wood (CFW) on the compressed side of the stem. However, the dose-effect responses of wood formation to repeated unidirectional bending treatments have not been established. In this study, we show that the number of bending events plays a crucial role in wood formation. To investigate this, young poplar stems were subjected to two different treatments involving different numbers of transient and unidirectional elastic bends. The radial growth of the stems was monitored throughout the treatments, and wood anatomy was quantitatively analysed and compared to control trees. The elliptic shape of poplar stem cross section, observed in response to the lowest dose, transformed into egg-shaped cross section in response to the highest dose. At the tissue level, the proportion of vessels vs fibers and their sizes were not differentially altered between the two treatments. However, there were notable differences in the proportion of G-fibers and the thickening of secondary cell walls, showing that the different traits of flexure wood have independent mechanosensitive control. Overall, our findings demonstrate that, in addition to their ability to respond to the intensity and direction of local mechanical strains, poplars adjust wood formation based on the number of bending events. These modifications likely enhance stem resistance against breakage when exposed to strong wind gusts.

Keywords Poplar · Mechanical stimuli · Strain · Dose-effect · Mechanosensitivity · Flexure wood · Bending · Wood anatomy · Secondary growth · Cell wall · G-layer · Thigmomorphogenesis

Introduction

The emergence of tissues providing a mechanical function was a key innovation for the colonization of the terrestrial environment by land plants. While for aquatic plants water buoys the plant body and offers mechanical support, land plants need to develop self-supporting aerial structures. For trees, as they often grow tall, slender, and stiff stems, their mechanical stability is constantly challenged by external mechanical loads, especially by wind-induced bending loads (Gardiner et al. 2016). Trees sense and acclimate to such mechanical stimulations by adjusting their growth and development, a process called thigmomorphogenesis (Jaffe 1973). In Greek, thigmo means 'to touch' and morphogenesis refers to the biological process that causes a tissue or organ to acquire its shape; thus, thigmomorphogenesis refers to touch-induced shape modifications. However, the use of this term has been extended to the effect of mechanical stimulations in general, and not merely restricted to touch stimulations. Thigmomorphogenesis has been observed in many dicotyledonous species (herbaceous and trees) and

Communicated by V. De Micco .

✉ Mélanie Decourteix
melanie.decourteix@uca.fr

[1] Université Clermont Auvergne, INRAE, PIAF, 63000 Clermont-Ferrand, France

[2] Université de Lorraine, AgroParisTech, INRAE, UMR Silva, 54000 Nancy, France

is usually characterized by a set of responses including a decrease in primary growth, an increased secondary growth, and a higher development of root anchorage (Telewski and Pruyn 1998; Coutand et al. 2008; Bonnesoeur et al. 2016). In nature, wind induces complex and repeated back and forth bending stimuli in many directions and with many frequencies (Rodriguez et al. 2008; Gardiner et al. 2016; Bonnesoeur et al. 2016). Analysing this thigmomorphogenetic syndrome mechanistically requires however simpler controlled and quantified bending stimulations. Unidirectional bending stimulations of controlled intensity are a key to this analysis. Biomechanical studies conducted on tomato and poplar demonstrated that the responses of primary growth (in tomato) and of secondary growth (in poplar) to bending stimulations are driven by the sensing of longitudinal mechanical strains. This relation has been formalized through the 'Sum of Strain Sensing' (S^3m) integrative model (Coutand and Moulia 2000; Coutand et al. 2009; Moulia et al. 2015). Beside such global effect on growth, it was observed that secondary growth is more highly stimulated in the direction of maximal mechanical stimulation. This was observed in response to bidirectional (back and forth) bending treatments (Telewski and Jaffe 1981 in *Pinus Taeda*; Telewski 1989 in *Abies fraseri*; Pruyn et al. 2000 in *Populus*). More recently, using unidirectional bending stimulations, Roignant et al. (2018) and Niez et al. (2019) demonstrated that, in the bent portion of the stem of young poplars, the secondary growth response is highly localized along the circumference of the cross section of the stem. Its intensity depends on the local intensity of the absolute value of longitudinal strains. Indeed, the cross section of poplar stem gets more elliptic as a result of an increased radial growth along the radii that experiences the highest longitudinal strains during bending. Using a finite-element modelling approach, Niez et al. (2019) demonstrated that such allocation of growth (and hence of wood biomass) along the bending direction increases both the stem bending rigidity and its resistance to breakage (strength) compared to a circular cross section with the same construction cost. These results validated the hypothesis that, although costly for the plants, thigmomorphogenesis is a crucial process for plants stability in a mechanically fluctuating environment.

The mechanical properties of a structure, like its bending strength, depend not only on the sizes of the structure, but also on the properties of the materials it is made of. Thus, mechanical properties of plant stems may depend on both its geometry and its tissues composition. In addition to changes in growth rates, changes in tissues composition are encountered in response to environmental cues. But the relation between external mechanical stimuli and plant responses at the tissue level has been overlooked in the literature. Regarding the effect of wind-related bending stimulations, the main efforts have been put into the study of wood formation. In a few genera such as *Abies* (Telewski 1989), *Pinus* (Telewski and Jaffe 1986) or *Populus* (Kern et al. 2005), multiple multidirectional bending treatments were shown to impact wood formation and to lead to the formation of a particular wood called "flexure wood" (Telewski 2016). To investigate the mechanisms involved in the response of cambial and wood cells to stem bending, unidirectional transient bending treatments of constant intensity were used (Roignant et al. 2018). In such experiments, a given cell is submitted to a maximal bending strain of constant intensity and sign (*i.e.* only compressive or tensile strain) at each successive bending stimulation. This has revealed that the wood formed under tensile flexural strains (Tensile Flexure Wood; TFW) differs from a wood formed under compressive flexural strains (Compressive Flexure Wood; CFW) (Roignant et al. 2018). Both share common anatomical deviations from normal wood. For example, in both types of flexure wood (TFW and CFW) vessel frequency is decreased, the diameter of wood fibres without a G-layer is increased and their cell wall thickness is increased. However, other anatomical traits are differentially modulated in Tensile and in Compressive Flexure Wood. Notably, the decrease in vessel diameter or the formation of a cell wall layer with typical features of a G-layer (Clair et al. 2018) in the fibres are specific to Tensile Flexure Wood (Roignant et al. 2018).

Altogether, it is now established that the absolute value of the intensity of the strains drives radial growth while a combination of the intensity and the sign of strains drives wood anatomy in response to bending. Moreover, several studies suggest the importance of taking the dose of stimulations during repeated stimuli into account. When considering a stem bending treatment, the dose can be described as the product of three parameters: (1) the frequency of recurrence of the stimulus, (2) the duration of the treatment (with frequency × duration determining the total number of stimuli), and (3) the intensity of the stimulus. A dose-response is thus an additive response to the sum of the intensity of each successive stimulus, accumulated over time. If the intensity of the stimulus is kept constant over-time, the response is linearly related to the number of stimulations. In species having an herbaceous or bushy growth habit, the main corpus of the studies on dose effects focused on responses to multiple unquantified stimuli such as rubbing or brushing (especially stem elongation inhibition, changes in biomass production or in flowering, Jaffe et al. 1980; Garner and Bjorkman 1996; Cipollini 1999; Morel et al. 2012), indicating that repeating the bending stimuli has an effect but precluding further analysis. In tree species, the consequences of multiple bending treatments on longitudinal and radial growth were studied in more details. Using varied numbers of bending treatments per days, Telewski and Pruyn (1998) compared the growth of the stems of non-staked *Ulmus americana* sapling to the growth of staked and non-staked but manually bent stems.

After 3 weeks of mechanical treatment, height growth was reduced in "non-staked control" trees compared to "staked control" trees and even more greatly reduced in trees manually flexed 5–80 times a day. Stem diameter was increased in manually bent and "non-staked control" trees compared to "staked control" trees. However, only the treatment made of 5 bending events per day significantly increased radial growth (when compared to non-staked control trees); there was no further additional secondary growth when the daily number of bending stimuli was further increased. In this study, although the lateral displacement of the tip of the stem was controlled, the applied strains were uncontrolled and unquantified. Indeed, as the applied strains strongly depend on the diameter of the bent stem (Moulia et al. 2015), even if the stems were bent with the same displacement of the stem tip all along the experiment, the intensities of strains were changing along as secondary growth was increasing the stem diameter (in both a time- and bending treatment-related ways). The study by Telewski and Pruyn (1998) thus revealed a complex effect of the repetition of bending; but their experimental protocol precluded further quantitative analysis of the dose-effect response. Later on, the effect of the dose was assessed by Coutand et al. (2009) using controlled bending-strain stimuli. They first studied the effect of the intensity of a single bending stimulus by varying the intensity of the strains. In this case, the responses of both (1) the radial growth and (2) the expression of *PtaZFP2*, a quantitative marker and major gene for the molecular response to bending, were highly correlated to the sum of longitudinal strains (integrated over the small portion of bent tissues) induced by the bending stimulus (Coutand et al. 2009; Martin et al. 2014). They then applied recurrent daily bending and found that the first three repeated bending events strongly increased radial growth compared to a single event, suggesting an additive model of dose-response. However, after the third bending, the additive effect was lost. These observations highlighted the existence of an accommodation process (Martin et al. 2010; Leblanc-Fournier et al. 2014; Moulia et al. 2015). This lead Martin et al. (2010) to propose an improved model (dose-accommodation model) in which the stem desensitizes after a dose of 3 bending at 2% maximal strain. Such 'accommodation' is thought to be crucial to avoid an over-response to recurrent stimulations like usual winds (Moulia et al. 2015; Bonnesoeur et al. 2016). However, this dose-accommodation model has never been assessed for repeated stimuli of more than one bending per day.

Consequently, there is still a lack of knowledge about the dose-response effect of repetitive bending on stem radial growth. This lack is even bigger when considering wood anatomy responses. Indeed, the formation of Tensile and Compressive Flexure Wood was only studied at the single frequency of 3 bending stimulations per week during 8 weeks (Roignant et al. 2018). We do not know if conclusions from this study are still relevant in the case of different stimulation regimes.

In this paper, we hypothesize that a higher number of bending stimulations may modify the wood formation responses (i.e., circumferential distribution of radial growth and Flexure Wood formation) previously observed in Roignant et al. (2018). Such responses may be linearly related (sensu stricto dose-dependent response) or not linearly related to the number of bending stimulations. Based on our knowledge of the desensitization of molecular and radial growth responses to repeated bending stimulations, we make the hypothesis that wood formation responses may be not strictly dose-dependent. The onset of an acclimative process may limit this dose-dependency to avoid non-acclimative over-responses. To test these hypotheses, we complemented the results published in Roignant et al. (2018) for radial growth and wood anatomy after 3 directional stimulations per week with results obtained after 15 stimulations per week, for 8 weeks. We applied unidirectional bending stimulations of controlled intensity which allowed us to assess heterogenous growth along the different radii of the cross section and to analyse both Compressive Flexure Wood and Tensile Flexure Wood.

Materials and methods

Plant material and culture conditions

Hybrid poplars (*Populus tremula* × *Populus alba*, clone INRA 717-1B4) were obtained by in vitro micropropagation on MS ½ medium (Murashige and Skoog 1962; Roignant et al. 2018). After acclimation, young trees were transferred to a greenhouse at 22 (± 1) °C (day) and 19 (± 1) °C (night) with a relative air humidity of 60 ± 10%, under natural light. The trees were planted in 4 l pots, in a substrate composed of one-third black peat and two-thirds local clay-humic Limagne soil (Bornand et al. 1975). Five months after micropropagation, the poplars were ready for the experiments. At that time, their stems had no branches and had a radius of about 6 mm at a height of 15 cm above the ground. Their average length was 68 cm (comprised between 48 and 84 cm). All trees were well watered throughout the experiment. One week before the first mechanical stimulations were applied, leaves were cut out from the basal part of the stem (control trees included), on a 30 cm long portion. Data were collected from two independent experiments (2015–2016), conducted during 8 weeks at the same period of the year (from May to July).

Mechanical stimulations

The choice of a range of frequencies of bending events was based on (1) the typical timing of wind events in the natural habitat of the plant species and (2) our knowledge of the accommodation capacities of poplar (Martin et al. 2010; Leblanc-Fournier et al. 2014). In a reference study of the power spectrum of horizontal wind kinetic energy in temperate climates of the northern hemisphere, Van der Hoven (1957) found two major eddy-energy peaks. The first one spans mostly from periods of approximately 2–8 days, with a maximum at a mean period of 4 days. It is related to the circulation of macro-meteorological cyclonic systems over the land. The second one spans mostly from periods of 1 s to 10 min with a maximum at a period of 1 min. It is related to the gusts of wind during a wind event. In between, there is a spectral gap from periods of 10 min to 3 h, for which there are almost no variation of wind kinetic energy due to wind eddies. From this analysis, we chose to define two sets of important parameters characterizing the artificial bending treatments:

(i) A number of days per week for which the trees are subjected to bending stimulations (representing the alternation of windy and calm weather due to macro-meteorological cyclonic events). For practical reasons, we retained two number of days: 3 days of bending treatments followed by 4 days without any bending treatment; that is 3 days of bending treatment per week, and 5 days of bending treatment followed by 2 days with no stimulation, i.e. 5 days of bending treatments a week. These two values frame the peak of period of macro-meteorological events, while providing a simple organization of the experimental work.

(ii) The number of successive bending events in a row during one day (i.e. during a simplified emulation of a micrometeorological storm event) and the time gap in between. We retained 1 bending stimulation per day and 3 bending stimulations per day. The maximal gap time in between successive bending was 3 h.

Thus, and to simplify the design, we only produced two extreme treatments noted 3-B/w and 15-B/w.

More precisely, the 3-B/w treatment consisted of a single unidirectional bend per day applied at 9 am on the basal part of the stem (30 cm), for three consecutive days per week (Monday–Wednesday) followed by full rest during 4 days (Roignant et al. 2018; Fig. 1a). This led to a total amount of 3 bends per week (acronomized 3-B/w). The 15-B/w treatment consisted of three unidirectional bending treatments per day (9 am, noon, and 3 pm) for five consecutive days per week (Monday–Friday) and full rest during 2 days, leading to a total amount of 15 bends per week (hence the acronym 15-B/w). The two treatments were applied during 8 weeks.

Growth conditions were identical for the 3-B/w and the 15-B/w treatments since both were carried out simultaneously, in the same greenhouse. The data for the low frequency treatment called "3-B/w" were the one published in Roignant et al. (2018).

The intensity of the bending treatment was controlled by a curved cylindrical plastic template providing a spatially homogeneous curvature (Roignant et al. 2018; Fig. 1). This geometrical configuration provided a strain field which is homogeneous along the longitudinal direction, and that varies linearly across the section of the stem (Coutand et al. 2009). Under these conditions, following the diameter of the stem (parallel to the direction of bending) (Fig. 1b), the longitudinal elastic strains increase from zero at the so-called "neutral line", up to the maximal strain intensity in the outer cell layer. Above and below the neutral line, strains intensities are equal but of different signs, as one part is submitted to tensile strains and the other to compressive ones.

For every tree and throughout the treatment period, we applied unidirectional transient bending treatments (Fig. 1a) with a maximum longitudinal strain of around 1% (the maximal non-injurious bending strain), and a duration of the loading–unloading cycle around 5 s. This high value of strain was retained in an attempt to emulate more complex loading during high but non-injurious wind events that were shown to be important for thigmomorphogenesis (Bonnesoeur et al. 2016). Trees were split up into three groups and submitted, or not, to mechanical treatments: 12 trees were submitted to the 3-B/w treatment; 12 trees were submitted to the 15-B/w treatment; 10 control trees grew without any mechanical stimulation. At the end of the treatment, the bent segment of each stem was cut into several parts: we distinguished the wood formed under tensile strains (stretched zone), under compressive strains (compressed zone), and the area called "neutral zone". The "neutral zone" surrounded the neutral line, which theoretically experienced no strain (see Fig. 1b and insert in the upper left corner, Fig. 4). Thus, tissues in the neutral zone experienced very little strains.

Growth analysis

During the treatment period, the stem diameters were measured weekly with a digital calliper in the direction of bending ($D_{//}$) and in the direction perpendicular to bending ($D_{\perp}$). $\Delta D_{//}$ corresponded to the growth in the direction where the applied longitudinal strain was the highest (ε_{max}), while $\Delta D_{\perp}$ corresponded to the neutral plane where the tissues experienced no mechanical strain. The resulting ovalization of the stem cross section was defined as in Roignant et al. (2018)

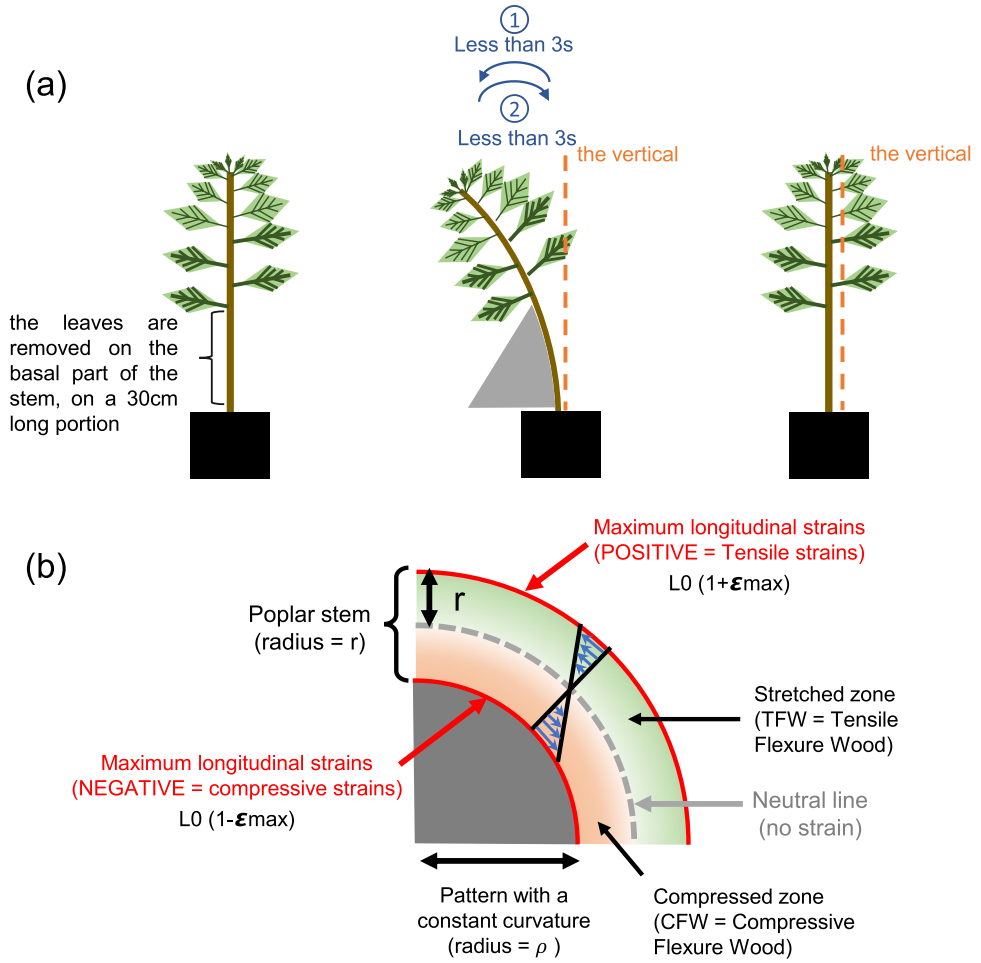

Fig. 1 Schematic representation of a bending treatment. **a** Leaves were removed on the basal part of the stem, on a 30 cm long portion. Then, the stem was unidirectionally bent on a template (portion of circle in dark grey). "Unidirectional bending treatment/stimulation" means (1) displacement from the upright position to one side against the template (duration is less than 3 s), followed by (2) a return to the original upright position (duration is less than 3 s). **b** Constant curvature of the template (quarter circle in dark grey) allows to impose a pure bending to the stem. For clarity purposes, the curvature of the template is much higher on the scheme than what was applied in the experiment. ρ is the radius of the curved pattern; r is the radius of the stem. The blue arrows represent the distribution of the intensities of longitudinal strains (either negative in the compressed zone, or positive in the stretched zone) along the diameter parallel to the bending direction. Maximal strain occurs at the periphery and its absolute value is equal to $\varepsilon = r/(r+\rho)$. εmax is the maximal strain applied to the stem (at the periphery of the stem, in the direction parallel to the bending direction). L0 is the initial length of the bent segment (30 cm). The 'neutral line' (dotted line in light grey) is a virtual line where longitudinal strain equals zero

$$\text{Oval}(t) = \frac{D_{//}(t)}{D_{\perp}(t)} \quad (1)$$

where t is time (in weeks). We define ovalization as the process whereby the axi-symmetrical round shape of the stem is changed to an oval shape; oval meaning a shape resembling either an egg or an ellipse.

Pith eccentricity

For both the control and the treated trees, the pith eccentricity, Ecc, was measured on stem cross sections at the end of the bending experiment. Stem segments were embedded in polyethylene glycol (PEG; molecular weight = 1500). Transverse Sections (25 µm-thick) were cut with a microtome

(LEICA RM 2165 rotary, Jena, Germany) and stained with 1% safranin–astra blue. Their visualization was performed on an Axio Observer Z1 microscope using Zen imaging software (Zeiss, Jena, Germany). Pith eccentricity represents the position of the pith along the diameter. The further the pith from the geometrical centre, the higher the eccentricity (*Ecc*). It was defined according to Lenz's formula (Lenz 1954; Roignant et al. 2018) as

$$\mathrm{Ecc}(\%) = \frac{e}{r} \times 100 \quad (2)$$

where e is the distance between the geometrical centre of the pith and geometrical centre of the stem cross section, and r is the mean radius of the stem cross section (computed with 60 rays). Eccentricity was taken as positive if the geometric centre of the cross section was on the side where wood was stimulated under tension and negative if the geometric centre was located on the side where wood was stimulated under compression.

Histological analysis

Histological analyses were realized as described in Roignant et al. (2018), on cross sections from stems that were sampled at the end of the bending experiment. Vessel diameter and vessel frequency measurements were realized on the images obtained for pith eccentricity (25 µm-thick cross sections, stained with 1% safranin astra-blue and visualized with an Axio Observer Z1 microscope using Zen imaging software (Zeiss, Jena, Germany)).

For the fibre cell wall measurements, small wood sticks were cut in the three sectors of interest, then fixed, dehydrated, and infiltrated with medium-grade LR white resin as described in Azri et al. (2009). Three to 4 µm thick sections were cut using an OmU2 rotary microtome (Reichert, Vienna, Austria) equipped with glass knives, and stained with 0.5% toluidine blue. Visualization of sections was performed on a Zeiss Axioskop 40 microscope using Zen imaging software (Zeiss, Jena, Germany).

The anatomical features (vessel diameter, vessel frequency, fibre diameter, G-fibre proportion, S-layer thickness, G-layer thickness) were measured with ImageJ software (Schneider et al. 2012). The results originate from the measurements of 20 cells (4 images per tree; 5 cells per image) per tree; this makes a total of 200–240 cells per experimental condition. The thickness of cell wall layers was measured on the samples embedded in LR white resin. Accurately distinguishing the primary wall layer with this technique remained difficult. Thus, we further refer to cell wall layers (excluding G-layer) with the terminology "S layer", merging the primary and S1–S2 layers. Moreover, to enhance contrast, photos were converted to greyscale.

Microfibril angle measurements

The mean microfibril angles (MFA) of the cell wall layers were determined as described in Roignant et al. (2018). Briefly, wood strips were sampled from debarked and oven-dried (48 h at 104 °C) portions of bent and unbent stems. The MFA of crystalline cellulose was measured at the SYLVATECH platform (INRAE, Nancy, France) with an X-ray diffractometer (Supernova, Oxford-Diffraction, Abingdon-on-Thames, UK). The evaluation of mean MFA was extracted from the 002 arc intensity curve using the method given in Verrill et al. (2006).

Statistical analysis

All measured and derived data were submitted to statistical analysis using R software (Team R. Core 2014). The normal distributions of the data were tested by the Shapiro–Wilk test. Analysis of variance (ANOVA) was used to determine whether anatomical parameters were significantly different or not. In the case of significant differences between bent trees and unbent trees, post-hoc analyses were based on the Tukey test.

Results

The number of bending treatments modulates the secondary growth non-linearly

The stem diameter in the direction parallel to the bending ($D_{//}$) was highly responsive to the number of bending stimulations since it was × 1.59 for 15-B/w and × 1.38 for 3-B/w

Table 1 Morphological dimensions of stems after 8 weeks of mechanical stimulations with the 3-B/w treatment (1 bending per day, 3 days per week) and the 15-B/w treatments (3 bending treatments per day, 5 days per week)

Morphological properties	Control	3-B/w	15-B/w
$\Delta D_{//}$ (mm)	5.8 ± 0.2^{a}	8.0 ± 0.2^{b}	9.2 ± 0.2^{c}
$\Delta D\perp$ (mm)	5.8 ± 0.2^{a}	6.5 ± 0.2^{a}	7.2 ± 0.2^{b}
Ovalization ($D_{//}/D\perp$)	1.01 ± 0.01^{a}	1.12 ± 0.01^{b}	1.14 ± 0.01^{b}
Pith eccentricity (%)	-0.4 ± 2.4^{a}	-4.8 ± 0.8^{a}	-6.4 ± 0.9^{b}

Means were obtained from the data of two independent experiments. Means (± s.e.) within each column with different letters are significantly different at $P < 0.05$ (ANOVA with a Tukey post-hoc test). $\Delta D_{//}$ and $\Delta D\perp$ are the total diameter increases in the direction parallel and perpendicular to the bending, respectively. Ovalization and pith eccentricity are computed according to Eqs. (1) and (2), respectively. In this table, ovalization is computed by dividing the diameter parallel to the bending direction by the diameter perpendicular to the bending direction (values measured after 8 weeks of mechanical stimulations). Data obtained with the 3-B/w treatment were published in Roignant et al. (2018)

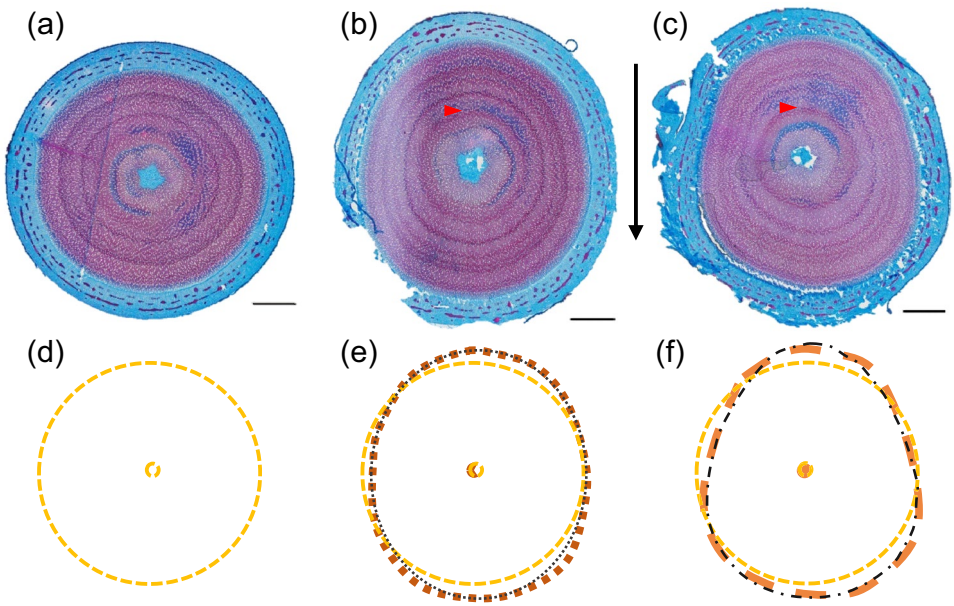

Fig. 2 Repeated unidirectional bending treatments result in an egg-shaped stem cross section. Cross section of *P. tremula*×*P. alba* without mechanical stimulation (**a**), after 8 weeks of 3-B/w bending treatment (**b**) and after 8 weeks of 15-B/w bending treatment (**c**). Staining: 1% safranin–astra blue. The black arrow shows the direction of bending and red arrows show the position of the cambium at the beginning of the mechanical treatments. **d**, **e**, **f** Shape of the section of the wooden region in bent stems is compared to the shape in control trees and to known geometrical shapes. **d** (Yellow dashed-line) manual circumferential outline of the wooden region and of the anatomical centers of the cross section of a control tree. **e** Circumferential outline of a control tree (yellow dashed-line) is superimposed with the circumferential outline (brown squared dashed-line) of 3-B/w trees and with an elliptic fit of the cross section (…). **f** Circumferential outline of a control tree (yellow dashed-line) is superimposed with the circumferential outline (orange dashed-line) of 15-B/w trees and with an ove-curve fit of the cross section (-.-). … elliptic fit of the cross section in (B) (equation $\left(\frac{x}{a}\right)^2+\left(\frac{y}{b}\right)^2=c^2$). -.- (egg-shaped) ove-curve fit of cross section in (C) (equation $\left(\frac{x}{a}\right)^2+\left(\frac{y}{(b+\beta x)}\right)^2=c^2$). Scale bar = 2 mm. Data obtained with the 3-B/w treatment were published in Roignant et al. (2018).

trees compared to control trees at the end of the 8 week-long treatment (Table 1, Fig. 2). This increase in final $D_{//}$ resulted from an almost systematic higher weekly radial increment in 15-B/w trees compared to control trees and 3-B/w trees (Fig. 3). However, even though bending treatments were 5 times more frequent in the 15-B/w than in the 3-B/w treatment, the response of the weekly radial increment was only 1.55 higher (mean over the 8 weeks). Thus, the radial increment response of the stem was non-linearly related to the frequency of the bending treatments.

The number of stimulations enforces a breakage of the elliptical symmetry of the growth response

While the diameter perpendicular to the direction of bending ($D_{\perp}$) was not impacted by the 3-B/w treatment, the 15-B/w trees presented a significantly higher $D_{\perp}$ (7.2 mm for 15-B/w vs 6.5 mm for 3-B/w trees) (Table 1).

Both treatments increased the global ovalization of the stem. However, the ovalization of the stem was not significantly modified between the two treatments (ovalization of 1.12 for the 3-B/w trees and 1.14 for the 15-B/w trees). Contrary to the 3-B/w treatment, we observed a significant negative pith eccentricity in response to the 15-B/w treatment, indicating that radial growth increment was higher in the compressed zone. This particular circumferential distribution of growth rate in 15-B/w trees leads to the formation of a stem with an egg-shaped cross section, instead of the elliptic cross section observed in 3-B/w trees (Fig. 2). To highlight this shift toward the elliptic- and egg-shaped cross section, we overlayed the actual shape of the wooden region of typical cross sections for each treatment (Fig. 2) with elliptic (Fig. 2e, -B/w treatment) or ove-curve fits (egg shape) (Fig. 2f, 15-B/w treatment) of these cross sections. The shape of the cross section obtained with the 15-B/w treatment matches the ove-curve fit. The shape of the cross section obtained with the 3-B/w

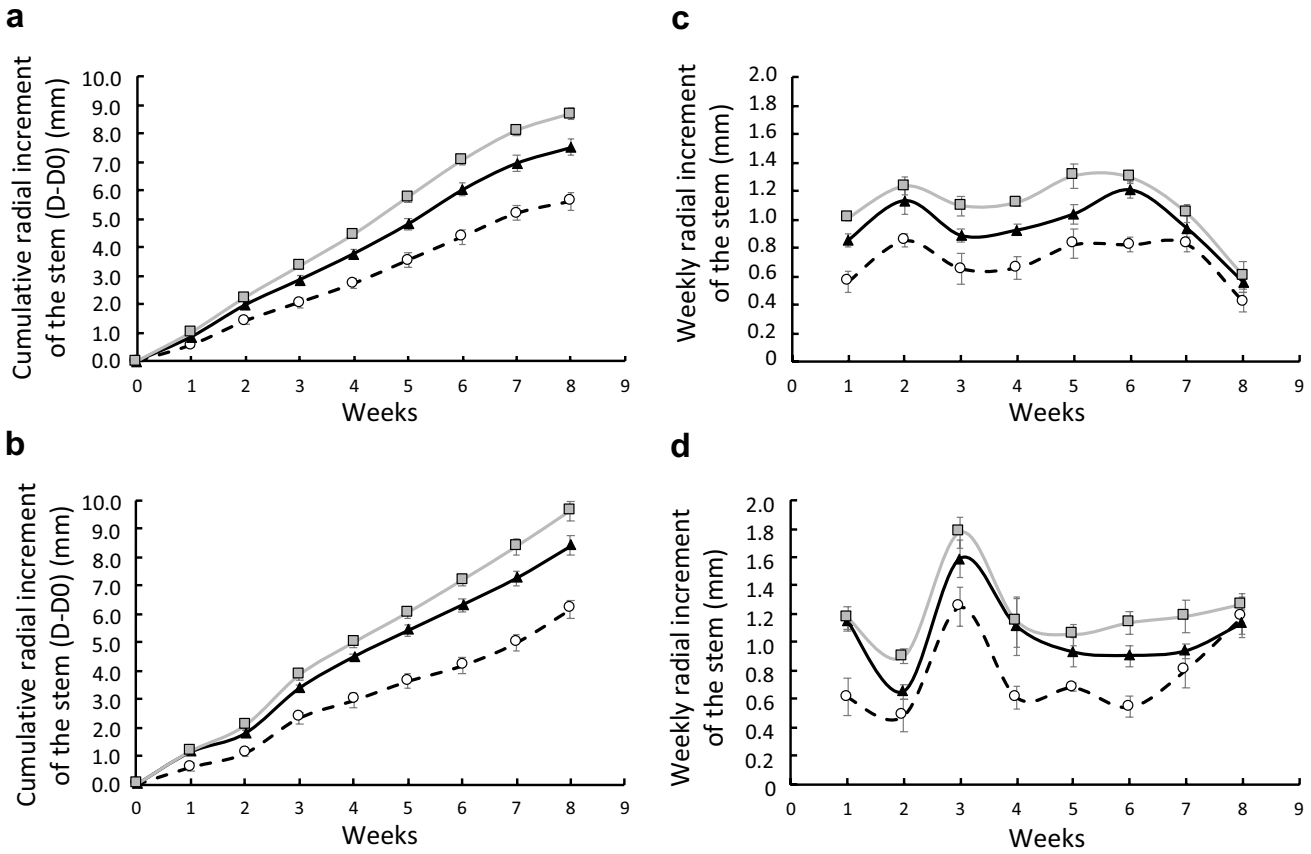

Fig. 3 Effect of the weekly frequency of bending on secondary growth. Cumulative radial increment of the stem of young poplar trees in response to different weekly frequencies of bending, in 2015 and 2016 (**a** and **b,** respectively). Weekly radial increment of the stem of young poplar trees in response to different weekly frequencies of bending, in 2015 and 2016 (**c** and **d,** respectively). Dotted lines refer to unbent (Ct) trees. Black triangles and grey squares refer to stems bent 3 times or 15 times a week, respectively. Vertical bars represent standard errors

Table 2 Modifications of anatomical traits of wood in different zones of bent poplar stems (stretched, neutral and compressed zones) in response to the 3-B/w and 15-B/w treatments

Anatomical properties	Control	Stretched zone		Neutral zone		Compressed zone	
		3-B/w	15-B/w	3-B/w	15-B/w	3-B/w	15-B/w
Vessel frequency (no. /mm^2)	187^{a}	151^{bc}	134^{c}	176^{a}	162^{ab}	151^{bc}	140^{c}
Vessel diameter (µm)	38 ± 0.7^{a}	34 ± 0.6^{b}	35 ± 0.6^{b}	37 ± 0.5^{a}	39 ± 0.3^{a}	37 ± 0.6^{a}	38 ± 0.7^{a}
Fibre diameter (µm)	13.9 ± 0.4^{a}	14.8 ± 0.4^{bc} 16 ± 0.3 (G)^{d}	14.9 ± 0.3^{bc} 16,3 ± 0.5 (G)^{d}	14.1 ± 0.3ab	14.5 ± 0.3^{ab}	14.9 ± 0.4^{bc}	15.4 ± 0.3 ^{cd}
G-fibre proportion (%)	1.9 ± 0.5^{a}	18.6 ± 1.8^{c}	31.9 ± 2.5^{d}	0.7 ± 0.1^{b}	0.9 ± 0.2^{b}	0.6 ± 0.1^{b}	0.6 ± 0.2^{b}
S-layer thickness (µm)	1.1 ± 0.03^{a}	1.3 ± 0.05 ^{cd} 0.79 ± 0.03 (G)^{f}	1.3 ± 0.03^{d} 0.77 ± 0.04 (G)^{f}	1.2 ± 0.02^{ab}	1.2 ± 0.05^{bc}	1.3 ± 0.06 ^{cd}	1.4 ± 0.03^{e}
G-layer thickness (µm)	–	1.16 ± 0.05^{a}	1.54 ± 0.8^{b}	–	–	–	
Microfibril angle (MFA) (°)	28^{a}	23^{b}	22^{b}	27^{a}	27^{a}	27^{a}	28^{a}

(G) refers to fibres with a G-layer. Means (± s.e.) within each column with different letters are significantly different at $P < 0.05$ (ANOVA with a Tukey post-hoc test). Data obtained with the 3-B/w treatment were published in Roignant et al. (2018)

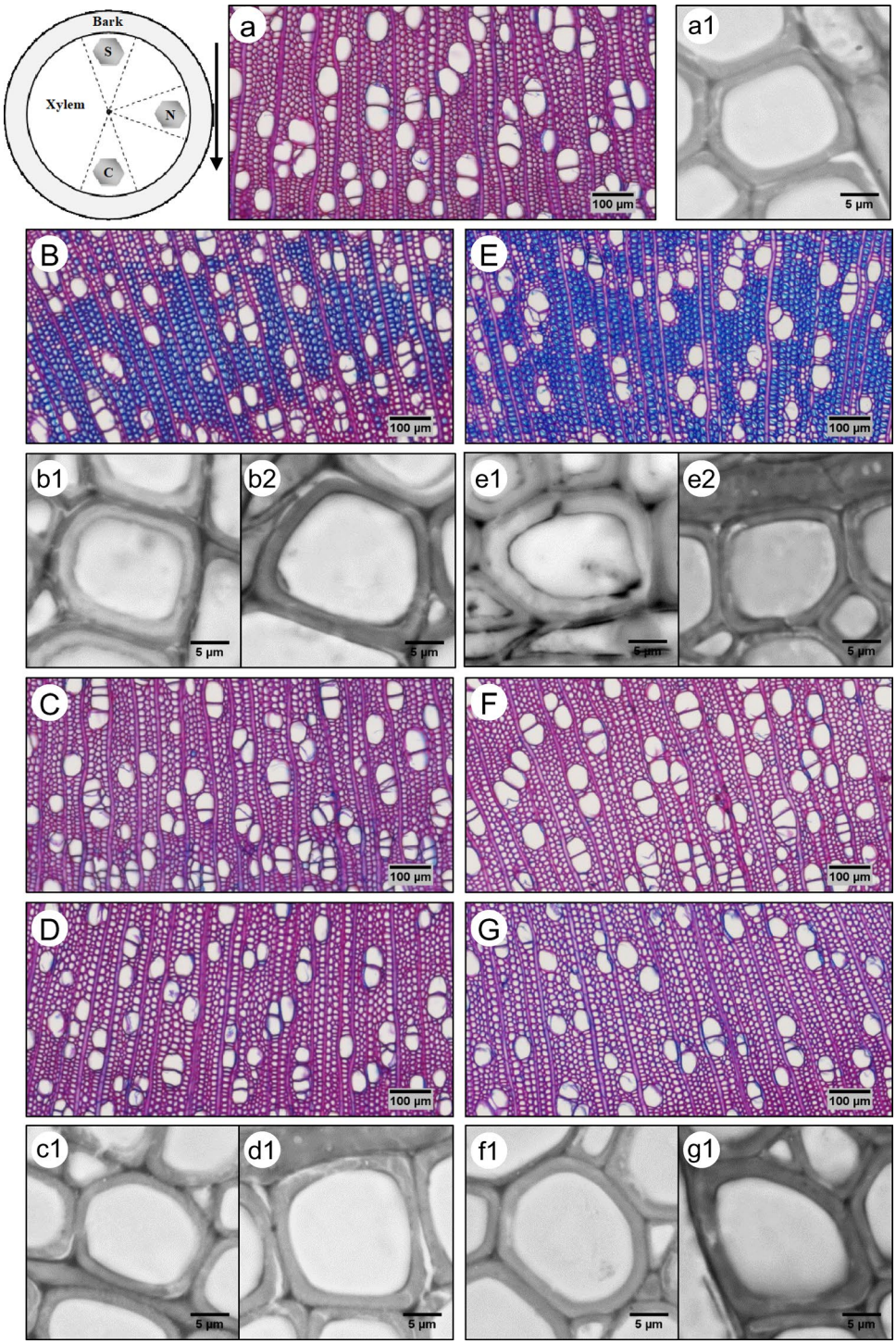

Fig. 4 Impact of the weekly frequency of bending on several wood anatomical traits. Anatomy details of *P. tremula*×*P. alba* without mechanical stimulation (**a**), after 8 weeks of 3-B/w bending treatment (**b–d**) and 15-B/w bending treatment (**e – g**). **b**, **e** Stretched zone; **c**, **f** Neutral zone; **d**, **g** Compressed zone. **a1**–**g1**; **b2** and **e2** Details of the cell wall fibres in wood of **a** control tree. **b1**, **b2**, **e1**, **e2** Stretched zone with **b1**, **e1** or without **b2**, **e2** a G-layer; **c1**, **f1** the neutral zone; **d1**, **g1** the compressed zone. **a**–**g** samples were collected and embedded in PEG, then cross sections were stained with 1% safranin–astra blue. **a1**–**g1**; **b2** and **e2** samples were collected and embedded in LR white resin, then cross sections were stained with toluidine blue, and photos were converted to grey scale

treatment matches the elliptic fit, except on the sides of the compressed zone where the shape of the cross section slightly departs from the elliptic fit.

Bending strains greatly influence the growth and differentiation of wood cells, and this response is non-linear with the number of bending stimulations

The effect of the two different bending treatments on wood anatomy was evaluated by measuring several anatomical traits in the compressed, neutral, and stretched

zones (Table 2, Fig. 4). The 15-B/w treatment drastically decreased the vessel frequency by 28% and 25% in the stretched and compressed zones, respectively, compared with control trees. However, these values were not significantly different from the results obtained with the 3-B/w treatment (− 19%). For both treatments, there was no effect of bending on vessel frequency in the neutral zone. Vessel diameter was impacted in the stretched zone of bent stems only. The 3-B/w and 15-B/w treatments had similar effects, with vessel diameter being 8.2% (3-B/w) and 7% (15-B/w) lower than in the control trees.

The proportion of fibres with a G-layer was responsive to the number of stretches. But this increase in the G-fibre frequency responded non-linearly to the number of bending as this proportion was only increased by × 1.72 while quintupling the number of bending. As with the 3-B/w trees, the compressed and neutral zones of the 15-B/w trees were devoid of G-fibres. Despite the higher number of fibres with a G-layer, the mean microfibril angle (MFA) was similarly reduced in the stretched zone of both treatments.

In 3-B/w stems, the diameter of fibres without G-layer was slightly higher in the stretched and compressed zones compared to fibres in the control trees. There was no significant difference with the neutral zone of bent trees. Similar results were observed in the 15-B/w trees, except in the compressed zone, where fibres diameter was higher compared to the neutral zone and the control trees. The diameter of fibres with a G-layer, measured in the stretched zone, was 15% higher than in fibres of control trees for both the 3-B/w and the 15-B/w treatments.

Bending strains influence the thicknesses of the secondary cell-wall layers in wood fibres

In 3-B/w trees, the mean S-layer thickness of fibres without G-layer (measured as the total of the S1 + S2 + S3 cell wall layers) was 10% thicker in the stretched and compressed zones compared to control trees (Roignant et al. 2018). In the 15-B/w trees, it was thicker in the stretched, neutral and compressed zones compared to the control. However, the cell wall thickness in the compressed zone was significantly thicker (1.38 µm; P value < 0,05) than in the neutral (1.22 µm) and the stretched (1.26 µm) zones. Moreover, while the S-layer in the stretched zone was identical between the two treatments, in the compressed zone of 15-B/w trees, the S-layer significantly increased compared to the compressed zone of 3-B/w trees, but only by 8%.

The S-layer of the G-fibres was identical between the 3-B/w and 15-B/w trees (0.79 µm and 0.77 µm, respectively) in the stretched zone. However, the G-layer was significantly thicker in 15-B/w trees (1.54 µm) compared to 3-B/w trees (1.16 µm) by 19%.

Discussion

The response of stem radial growth to the cumulated number of bending: more than longitudinal strain sensing

In trees, applying high doses of bending stimulations may reveal that the response of stem radial growth is more complex than was first proposed. Experimental data combined with modelling approaches showed that stem radial growth is influenced by the local intensity of longitudinal strains (in absolute value) (Coutand et al. 2009; Moulia et al. 2015), at every position around the cambium (Roignant et al. 2018; Niez et al. 2019). So, it was argued that this could explain why the growth stimulations in the stretched and compressed part of the stem were identical, leading to an elliptic shape of the cross section. However, the egg-shaped cross section and the negative pith eccentricity observed with the 15-B/w treatment showed that the sensitivity to the absolute value of the intensity of longitudinal strains is not sufficient to explain the growth response for high stimulation amounts.

A first explanation to the onset of an egg-shaped cross section could be that, besides the number of longitudinal strains, radial elastic strains linked to Poisson's ratio may also be influential. Basically, Poisson's ratio for elastic behaviour involves a lateral shrinkage where the tissue is stretched longitudinally, and a lateral expansion where it is compressed (see Fig. 4a in Faroughi and Shaat 2018). When the stem is bent, in the zone that is longitudinally compressed, cell walls may undergo Poisson's elastic stretching in the radial and tangential directions. As cell wall expansion is known to be powered by tensile stretching (Geitmann and Ortega 2009), Poisson's stretching may enhance radial and circumferential growth. However, assessing this hypothesis would require a detailed and complex analysis of the elastic strain of the cross section during bending. A second explanation could be that radial growth is responsive to both the intensity and the sign of the longitudinal strains, again to be challenged through a detailed biomechanical study.

Whatever the explanatory mechanism behind this behaviour, a question remains: How could one then explain the elliptic shape (absence of egg shape) of the cross section in the 3-B/w treatment? Although an effect of the frequency of bending treatments on growth responses of the stem cannot be ruled out, it is possible that the 3-B/w treatment also initiated an egg shape, without us being able to identify it. Indeed, an incipient trend toward egg-shaping seems likely from Fig. 2e. Egg-shaping would thus be always present, but its amount would depend on the bending dose. To fully test this hypothesis, it would be interesting to verify if applying the 3-B/w treatment for a longer period of time, or if

applying the same regime with a higher strain intensity, could lead to a clear egg-shaped cross section too.

Growth accommodates to repeated mechanical loads

Thigmomorphogenetic growth responses to bending stimulations could be of dose type or of accommodation type involving changes in the mechanical sensitivity along the repetitive loading. A dose-type response entails additive response to the cumulated number of stimuli. In other words, if the intensity of the stimulations is kept constant, the response is linearly related to the number of stimulations. On the contrary, a response of an accommodation type entails a non-linear response. Additionally, the response may even involve a specific frequency effect (that is an effect of frequency for the same cumulated number of stimuli). Experiments conducted on poplar stem led to the design of a dose-accommodation model for radial growth (Martin et al. 2010), providing the first evidence of a tuning of the sensitivity to mechanical stimulations along stimulus history. In our experiments, the response of radial growth was not linearly related to the total number of bending stimulations since radial growth was only 1.15 times higher (15-B/w vs 3-B/w) when trees were treated with five times more bending. This falsifies a pure dose-response model and confirms the ability of young poplar stems to accommodate the response of their secondary growth to recurrent bending treatments with different bending regimes, as already observed by Martin et al. (2010). In Martin et al. 2010, the desensitization was achieved after a strain dose of $3 \times 2\% = 6\%$, by applying 3 bending stimulations with a strain intensity of 2%. In our experiments, the strain intensity was 1% so that a dose of 6% was achieved with 6 bending stimulations. Since this dose is weekly exceeded with the 15-B/w treatment but not yet reached with the 3-B/w treatment, the dose-accommodation model (Martin et al. 2010) predicts that the 15-B/w treatment would lead to a higher growth stimulation than the 3-B/w treatment, which matches our results. Hence, our results falsify the pure dose-response model but do not falsify the dose-accommodation model. However, further mechanistic investigations, reviewed in Leblanc-Fournier et al. (2014), have revealed that the accommodation process at the molecular level starts up very early after a bending stimulation and that the timing for its building up has to be taken into account (besides the simplistic idea of a bending counting process). Therefore, additional experiments are now needed to fully explore how bending amount and timing control stem sensitivity to bending.

Beyond accommodation to successive repeated bending stimulations, another important aspect is the time to recover full sensitivity, so to characterize the entire desensitization–resensitization cycle. In Martin et al. (2010), it took more than 7 days for poplar stem to recover gradually its full growth response capacity. In our experiments, desensitization–resensitization cycles seemed to operate on shorter time scales (< 1 week) since radial growth of poplars responded to each set of weekly bending stimulations without attenuation during the 8 weeks of treatment. Thus, our results demonstrate for the first time that the number of bending may influence the kinetics of the desensitization–resensitization processes. Important research efforts are now needed to specify more accurately this kinetics along the repeated stimuli and to concurrently unravel the mechanisms underlying poplar stem sensitivity to bending.

Cell wall formation responds to the increased number of stimulations, whereas cell fate and growth do not. But all may follow an accommodation-type model

In addition to radial growth, the formation of Flexure Wood could respond to an increased number of bending stimulations following an accommodation-type model and not a pure a dose-type model.

G-layer formation and thickening processes seem to respond more strongly to an increased number of stimulations, but responses again follow an accommodation-type model. Roignant et al. (2018) showed that about 18% of wood fibres in the stretched zone of 3-B/w trees presented the development of a G-layer. Here, we show that this proportion was highly increased up to 31.9% in response to the 15-B/w treatment. Moreover, in G-fibres of the 15-B/w trees, the G-layer was thicker than in 3-B/w trees. However, the proportion of fibres developing a G-layer and the thickness of the G-layer are non-linearly related to the number of bending stimulations. Hence, some but not all extra-bending stimulations in the 15-B/w treatment (compared to the 3-B/w treatment) may lead to a response. Thus, sensitivity accommodation may apply to G-layer formation too.

Not all aspects of wood anatomy may respond to an increased number of stimulations as G-layer do. Histological analysis pointed out that S-layer in fibres developing a G-layer, vessel frequency, vessel diameter and fibre diameter responded similarly to the two bending treatments (3-B/w and 15-B/w). For the last three anatomical features, this could be explained either by saturation of the response or by the desensitization process, as already discussed for radial growth. For the S-layer, the timing of recurrent stimulations could be involved. Fang et al. (2007, 2008) observed a negative correlation between G-layer thickness and S-layer thickness. In their conditions, when G-layer thickness increased, S-layer decreased. In our study, the S-layer of G-fibres was decreased too in comparison to the S-layer of fibres in control trees. However, even if the G-layer was thicker in the 15-B/w TFW, the S-layer thickness of fibres developing

a G-layer remained identical between the two treatments. Altogether, we can propose the following qualitative model: (1) stem bending would trigger G-layer initiation and more frequent/numerous stimulations may activate the transcriptional program that is necessary for G-layer formation in a higher number of fibres; (2) this initiation would cancel S-layer development as suggested by Fang et al. (2007; 2008); (3) in the 15-B/w treatment, the time between two successive bending treatments would be short enough for the process of G-layer deposit to be reactivated or prolonged (in a given fibre) in response to a new bending stimulus, thus conducting to an increased G-layer thickness.

Increasing the amount of repeated bending stimulations reveals new abilities of cells to respond—an adaptive benefit?

The mechanical properties of a tree stem depend on both its geometry and the intrinsic wood properties. Considering two stems of different diameters made of a similar material, the thinner one is more flexible than the thicker one with a dependency on the 4th power of the radius. The higher increment of the diameter of 15-B/w stems compared to 3-B/w stems could be considered as the very first steps of an adaptive advantage for trees: thanks to allometric changes, the stem would become more rigid and more resistant to breakage when bent more frequently, so when the risk of breakage increases. Moreover, we noticed that the very first signs of a transition toward an egg shape can be observed at the end of the 3-B/w treatment, while the final shape of the 15-B/w stems exhibited a clearer egg shape, characterized by a wider section in the compression zone. Similar but more pronounced shape modifications have been observed in poplar stems exposed to a 15 B/w bending treatment of similar strain intensity (1%) over a × 2.5 longer period of time (5 months instead of 8 weeks). In their theoretical mechanical analysis, Niez et al. (2019) suggested that such an asymmetrical shape, with more biomass allocated in the compression side, modifies the stress distribution in the transversal cross section and improves the mechanical safety of the stem. Given that ruptures occur more easily when wood experiences compression than when it is stretched, Niez et al. (2019) demonstrated that allocating biomass preferentially in the side under compression is a relevant strategy for the mechanical resistance of the stem that constitutes an adaptive benefit when the tree encounters external mechanical loadings. Our results show that for a similar duration, increasing the number of bending hastens the ovalization of the stem toward the egg shape. Thereby, increased repeated stimulations could accelerate the adaptative plastic response of the tree.

In addition to geometry, the mechanical properties of the stem tissues, wood and bark, contribute to the overall mechanical behaviour of a stem. For wood, longitudinal stiffness as well as longitudinal strength is positively correlated with the basic density and negatively correlated with microfibril angle (MFA) (Evans and Ilic 2001; Yang and Evans 2003; Niez et al. 2020). The higher increase in the thickness of fibres cell wall layers in the zones experiencing maximal strains (G-layer in the stretched zone and S-layer in the compressed zone), while keeping both the diameter of the fibres and the MFA almost unchanged, suggests an improved mechanical stiffness and strength of these tissues especially in the compressed zone of 15-B/w trees. The combination of the mechanical reinforcement resulting both from the secondary growth (elliptical and egg shape reducing bending stresses through their effect on the second moment of area) and modifications of wood anatomy (increased cell wall thickness decreasing bending stress and increasing the resistance to cell-wall buckling) may improve the weak point of the stem in compression during a bending event, as recently suggested by Jacobsen et al. (2005) and Niez et al. (2019, 2020).

Conclusion

Trees can perceive mechanical strains, allowing them to adjust their shape and tissue mechanical resistance to repetitive bending stimulations. In the case of unidirectional bending, poplar trees produce special types of wood: Tensile Flexure Wood (TFW) on the stretched side, and Compressive Flexure Wood (CFW) on the compressed side of the stem. Here we showed that secondary growth responds to multiple stimulations according to the number of bending. The control of every parameter of the dose of stimulation allowed to disentangle the effect of strain intensity from the number of stimulations. This highlighted that a high number of stimulations leads to a non-linear response of secondary growth, especially in the region under compression. It also emerged from anatomical analyses that processes related to cell wall formation, like G-layer initiation and G-layer thickness in the TFW, depends on the number of stimulations (again non-linearly) whereas processes related to cell fate determination and growth do not. Our results highlighted the complexity of poplar stem responses to repeated bending stimulations. They open new questions on the ability of trees to adjust their sensitivity to mechanical loadings depending on their amount and recurrence. A dynamic interplay between modelling and experimental approaches is now needed to progress in our understanding of this accommodation phenomenon.

Author contribution statement JR[1], MD and EB contributed to the study conception and design. JR[2] performed the MFA

measurements with the technical help of JR[1]. JR[1] and NBM performed all the other experiments. Data analysis was performed by JR[1]. The first draft of the manuscript was written by JR[1] and MD. All the authors contributed to the writing of the final version of the manuscript.

Acknowledgements We thank Christelle Boisselet, Patrice Chaleil, Aline Faure, Jérôme Franchel, Caroline Savel, Brigitte Girard, Stéphane Ploquin for their technical help. The authors would also like to thank SILVATECH (Silvatech, INRAE, 2018. Structural and functional analysis of tree and wood Facility, https://doi.org/10.15454/1.5572400113627854E12) from UMR 1434 SILVA, 1136 IAM, 1138 BEF and 4370 EA LERMAB EEF research center INRAE Nancy-Lorraine for the measurements of microfibril angle.

Funding This work was supported by grants from the Auvergne Regional Council ("Programme Nouveau Chercheur de la Région Auvergne-2014") and from CNES (Centre National d'Etudes. Spatiales). SILVATECH facility is supported by the French National Research Agency through the Laboratory of Excellence ARBRE (ANR-11-LABX-0002–01).

Data availability The datasets generated during and/or analysed during the current study are available from the corresponding author on reasonable request.

Declarations

Conflict of interest The authors have no relevant financial or non-financial interests to disclose.

References

Azri W, Chambon C, Herbette S, Brunel N, Coutand C, Leplé JC, Ben Rejeb I, Ammar S, Julien J-L, Roeckel-Drevet P (2009) Proteome analysis of apical and basal regions of poplar stems under gravitropic stimulation. Physiol Plant 136:193–208. https://doi.org/10.1111/j.1399-3054.2009.01230.x

Bonnesoeur V, Constant T, Moulia B, Fournier M (2016) Forest trees filter chronic wind-signals to acclimate to high winds. New Phytol 210:850–860. https://doi.org/10.1111/nph.13836

Bornand M, Dejou J, Servant J (1975) Les terres noires de limagne; leurs différents faciès et leur place dans la classification française des sols. Comptes Rendus L'académie Des Sci Série D 281:1689–1692

Cipollini DF (1999) Costs to flowering of the production of a mechanically hardened phenotype in *Brassica napus L.* Int J Plant Sci 160:735–741. https://doi.org/10.1086/314164

Clair B, Déjardin A, Pilate G, Alméras T (2018) Is the G-layer a tertiary cell wall? Front Plant Sci 8:9–623. https://doi.org/10.3389/fpls.2018.00623

Coutand C, Moulia B (2000) Biomechanical study of the effect of a controlled bending on tomato stem elongation: local strain sensing and spatial integration of the signal. J Exp Bot 51:1825–1842. https://doi.org/10.1093/jexbot/51.352.1825

Coutand C, Dupraz C, Jaouen G, Ploquin S, Adam B (2008) Mechanical stimuli regulate the allocation of biomass in trees: demonstration with young prunus avium trees. Ann Bot 101:1421–1432. https://doi.org/10.1093/aob/mcn054

Coutand C, Martin L, Leblanc-Fournier N, Decourteix M, Julien J-L, Moulia B (2009) Strain mechanosensing quantitatively controls diameter growth and PtaZFP2 gene expression in poplar. Plant Physiol 151:223–232. https://doi.org/10.1104/pp.109.138164

Evans R, Ilic J (2001) Rapid prediction of wood stiffness from microfibril angle and density. For Prod J 51:53–57

Fang CH, Clair B, Gril J, Alméras T (2007) Transverse shrinkage in G-fibers as a function of cell wall layering and growth strain. Wood Sci Technol 41:659–671

Fang CH, Clair B, Gril J, Liu SQ (2008) Growth stresses are highly controlled by the amount of G-layer in poplar tension wood. IAWA J 29:237–246. https://doi.org/10.1007/s00226-007-0148-3

Faroughi S, Shaat M (2018) Poisson's ratio effects on the mechanics of auxetic nanobeams European. J Mech A/Solids. https://doi.org/10.1016/j.euromechsol.2018.01.011

Gardiner B, Berry P, Moulia B (2016) Review: wind impacts on plant growth, mechanics and damage. Plant Sci 245:94–118. https://doi.org/10.1016/j.plantsci.2016.01.006

Garner LC, Björkman T (1996) Mechanical conditioning for controlling excessive elongation in tomato transplants: sensitivity to dose, frequency, and timing of brushing. J Am Soc Hortic Sci 121:894–900. https://doi.org/10.21273/JASHS.121.5.894

Geitmann A, Ortega JKE (2009) Mechanics and modelling of plant cell growth. Trends Plant Sci 14:467–478. https://doi.org/10.1016/j.tplants.2009.07.006

Jacobsen AL, Ewers FW, Pratt RB, Paddock WA, Davis SD (2005) Do xylem fibers affect vessel cavitation resistance? Plant Physiol 139:546–556. https://doi.org/10.1104/pp.104.058404

Jaffe MJ (1973) Thigmomorphogenesis: the response of plant growth and development to mechanical stimulation. Planta 114:143–157. https://doi.org/10.1007/BF00387472

Jaffe MJ (1980) Morphogenetic responses of plants to mechanical stimuli or stress. Bioscience 30:239–243. https://doi.org/10.2307/1307878

Kern KA, Ewers FW, Telewski FW, Koehler L (2005) Mechanical perturbation affects conductivity, mechanical properties and aboveground biomass of hybrid poplars. Tree Physiol 25:1243–1251. https://doi.org/10.1093/treephys/25.10.1243

Leblanc-Fournier N, Martin L, Lenne C, Decourteix M (2014) To respond or not to respond, the recurring question in plant mechanosensitivity. Front Plant Sci 5:401. https://doi.org/10.3389/fpls.2014.00401

Lenz O (1954) Le Bois de quelques peupliers de culture en Suisse ETH Zurich

Martin L, Leblanc-Fournier N, Julien J-L, Moulia B, Coutand C (2010) Acclimation kinetics of physiological and molecular responses of plants to multiple mechanical loadings. J Exp Bot 61:2403–2412. https://doi.org/10.1093/jxb/erq069

Martin L, Decourteix M, Badel E, Huguet S, Moulia B, Julien JL, Leblanc-Fournier N (2014) The zinc finger protein PtaZFP2 negatively controls stem growth and gene expression responsiveness to external mechanical loads in poplar. New Phytol 203:168–181. https://doi.org/10.1111/nph.12781

Morel P, Crespel L, Galopin G, Moulia B (2012) Effect of mechanical stimulation on the growth and branching of garden rose. Sci Hortic 135:59–64. https://doi.org/10.1016/j.scienta.2011.12.007

Moulia B, Coutand C, Julien J-L (2015) Mechanosensitive control of plant growth: bearing the load, sensing, transducing, and responding. Front Plant Sci. https://doi.org/10.3389/fpls.2015.00052

Murashige T, Skoog F (1962) A revised medium for rapid growth and bio assays with tobacco tissue cultures. Physiol Plant 15:473–497. https://doi.org/10.1111/j.1399-3054.1962.tb08052.x

Niez B, Dlouha J, Moulia B, Badel E (2019) Water-stressed or not, the mechanical acclimation is a priority requirement for trees. Trees 33:279–291. https://doi.org/10.1007/s00468-018-1776-y

Niez B, Dlouha J, Gril J, Ruelle J, Toussaint E, Moulia B, Badel E (2020) Mechanical properties of "flexure wood": compressive stresses in living trees improve the mechanical resilience of Wood and its resistance to damage. Ann for Sci 77:17. https://doi.org/10.1007/s13595-020-0926-8

Pruyn ML, Ewers BJ, Telewski FW (2000) Thigmomorphogenesis: changes in the morphology and mechanical properties of two populus hybrids in response to mechanical perturbation. Tree Physiol 20:535–540. https://doi.org/10.1093/treephys/20.8.535

Rodriguez M, de Langre E, Moulia B (2008) A scaling law for the effects of architecture and allometry on tree vibration modes suggests a biological tuning to modal compartmentalization. Am J Bot 95(12):1523–1537. https://doi.org/10.3732/ajb.0800161

Roignant J, Badel E, Leblanc-Fournier N, Brunel-Michac N, Ruelle J, Moulia B, Decourteix M (2018) Feeling stretched or compressed? the multiple mechanosensitive responses of wood formation to bending. Ann Bot 121:1151–1161. https://doi.org/10.1093/aob/mcx211

Schneider CA, Rasband WS, Eliceiri KW (2012) NIH image to imageJ: 25 years of image analysis. Nat Methods 9:671–675. https://doi.org/10.1038/nmeth.2089

Team R. Core (2014) *R:* A language and environment for statistical computing. R foundation for statistical computing, Vienna, Austria. 2013. ISBN 3–900051–07–0.

Telewski FW (1989) Structure and function of flexure wood in Abies fraseri. Tree Physiol 5:113–121. https://doi.org/10.1093/treephys/5.1.113

Telewski FW, Jaffe MJ (1981) Thigmomorphogenesis: changes in the morphology and chemical composition induced by mechanical perturbation in 6 month old pinus taeda seedlings. Can J for Res 11:380–387. https://doi.org/10.1139/x81-051

Telewski FW, Jaffe MJ (1986) Thigmomorphogenesis: anatomical, morphological and mechanical analysis of genetically different sibs of pinus taeda in response to mechanical perturbation. Physiol Plant 66:219–226. https://doi.org/10.1111/j.1399-3054.1986.tb02412.x

Telewski FW, Pruyn ML (1998) Thigmomorphogenesis: a dose response to flexing in *Ulmus americana* seedlings. Tree Physiol 18:65–68. https://doi.org/10.1093/treephys/18.1.65

Telewski FW (2016) Flexure Wood: Mechanical Stress Induced Secondary Xylem Formation In: Secondary Xylem Biology. Elsevier https://doi.org/10.1016/B978-0-12-802185-9.00005-X

Van der Hoven I (1957) Power spectrum of horizontal wind speed in the frequency range from 0.0007 to 900 cycles per hour. J Meteorol 14:160–164. https://doi.org/10.1175/1520-0469(1957)014<0160:PSOHWS>2.0.CO;2

Verrill SP, Kretschmann DE, Herian VL (2006) JMFA2 – a graphically interactive Java program that fits microfibril angle X-ray diffraction data. Research Paper FPL-RP-635. US Department of Agriculture, Forest Service, Forest Products Laboratory. Madison, WI. https://doi.org/10.2737/FPL-RP-635

Yang JL, Evans R (2003) Prediction of MOE of eucalypt wood from microfibril angle and density. Holz Als Roh-und Werkstoff 61:449–452. https://doi.org/10.1007/s00107-003-0424-3